Wi-Fi 6E Mesh Networks

Where To Place The Extenders?

Ramírez-Arroyo, Alejandro; Damsgaard, Sebastian Bro; Berardinelli, Gilberto; Sørensen, Troels B.; Mogensen, Preben; Kaagaard, Jesper

Published in:
2024 IEEE 100th Vehicular Technology Conference (VTC2024-Fall)

DOI (link to publication from Publisher):
10.1109/VTC2024-Fall63153.2024.10757459

Publication date:
2024

Document Version
Early version, also known as pre-print

Wi-Fi 6E Mesh Networks: Where To Place The Extenders?

Alejandro Ramírez-Arroyo*, Sebastian Bro Damsgaard*, Gilberto Berardinelli*,
Troels B. Sørensen*, Preben Mogensen*†, Jesper Kaagaard‡
*Department of Electronic Systems, Aalborg University (AAU), 9220 Aalborg, Denmark;
(e-mails: araar@es.aau.dk; sbd@es.aau.dk; gb@es.aau.dk; tbs@es.aau.dk; pm@es.aau.dk)
†Nokia, 9220 Aalborg, Denmark (e-mail: preben.mogensen@nokia.com)
‡Sky Labs Aalborg, 9000 Aalborg, Denmark (e-mail: jesper.kaagaard@sky.uk)

Abstract—**Wi-Fi is one of the WLANs technologies with the highest penetration in society worldwide. In recent years, Wi-Fi 6E has been defined, which uses the 6 GHz band with higher bandwidth and resource availability. However, the range for this band decreases due to the increase in frequency compared to 2.4 GHz and 5 GHz bands, hence the proposal for the use of mesh networks to overcome the limited range. Therefore, this work empirically assesses the network performance through different setups in indoor scenarios to determine the optimal placement of extender nodes in a Wi-Fi 6E mesh network. The experimental methodology follows a dual approach, studying the channel propagation conditions in the 6 GHz band versus 2.4 GHz and 5 GHz, as well as the throughput reported through connectivity with Wi-Fi 6E. The results quantitatively show the reduction in effective network range in the 6 GHz band, due to the increase in frequency, and its influence on effects such as blocking or around-corner propagation. Based on this analysis, a set of guidelines is developed for positioning the extender nodes in the network to maximize network performance according to the propagation channel conditions.**

Index Terms—**Measurements, mesh networks, propagation, throughput, Wi-Fi 6E.**

I. Introduction

Wireless Local Area Networks (WLANs) have had an essential impact on the development and access to the Internet [1]. Among the best-known WLANs are the set of protocols popularly known as Wi-Fi. Wi-Fi networks, originally released in 1997 with a throughput of up to 2 Mbps, are standardized in the IEEE 802.11 standards [2]. While in 1997 these 2 Mbps were reasonable for Internet access, the evolution of network services is clearly insufficient for current user needs. For instance, streaming, gaming, or cable television services require higher bandwidths. Therefore, Wi-Fi technology and IEEE 802.11 standards have had to adapt over time to suit the user requirements.

In order to improve the network performance, Wi-Fi has introduced several improvements in terms of (i) modulation and transmission schemes [3] and (ii) frequency bands and bandwidth available [4], allowing data rates up to Gbps nowadays. Concerning the modulation schemes, for instance, direct-sequence spread spectrum/complementary code keying (DSSS/CCK) was implemented in IEEE 802.11b (Wi-Fi 1), while orthogonal frequency-division multiplexing (OFDM) was supported starting by IEEE 802.11a (Wi-Fi 2). Regarding the frequency bands, Wi-Fi was originally developed to operate on the unlicensed 2.4 GHz. In 1999, Wi-Fi 2 proposed the use of the 5 GHz band, which became popular and nowadays coexists alongside the 2.4 GHz band in the IEEE 802.11n/ac/ax standards (Wi-Fi 4, Wi-Fi 5, and Wi-Fi 6). Finally, in 2020 Wi-Fi 6E was adopted as an extension of the IEEE 802.11ax standard [5]. This technology stands out mainly for the incorporation of the 6 GHz band [6]. This fact is critical from the bandwidth availability perspective. Due to the penetration of Wi-Fi technology in the market, the 2.4 GHz band (and to a lesser extent 5 GHz) has multiple sources of interference due to the high density of access points (AP) in indoor environments and the low number of available channels [7]. This interference between APs degrades the performance of Wi-Fi networks by decreasing the achievable data rate. Thus, the main objective of Wi-Fi 6E is to enable denser networks where multiple devices can cohabit while avoiding inter-channel interference. The 6 GHz band in Europe is located from 5925 MHz to 6425 MHz (500 MHz bandwidth), also offering flexibility in the available channel bandwidth for transmission, ranging from 20 MHz to 320 MHz. All these features theoretically enable a considerable increase in bandwidth compared to the 2.4 GHz and 5 GHz bands. Despite all these advantages, this band also has some limitations. From the point of view of radio propagation, the usage of high carrier frequencies limits the operating range of WLANs due to increased path loss [8]. Similarly, the presence of obstacles affects the 5 GHz and 6 GHz bands more than 2.4 GHz band because the shorter wavelength makes the signal more prone to blocking.

For the above reasons, finding a solution to increase the effective range of Wi-Fi 6E networks is necessary so that network performance can be preserved with an extended range. For instance, this extended range would enable the streaming of high-quality video over a Wi-Fi network with large coverage area. One of the most commercially successful proposals is the use of mesh wireless networks, which are composed of interconnected nodes that are transparent to the end user [9]. Despite the presence of multiple APs, these networks act as if they were a single WLAN with a large range compared to a network scheme with a single AP. Under the

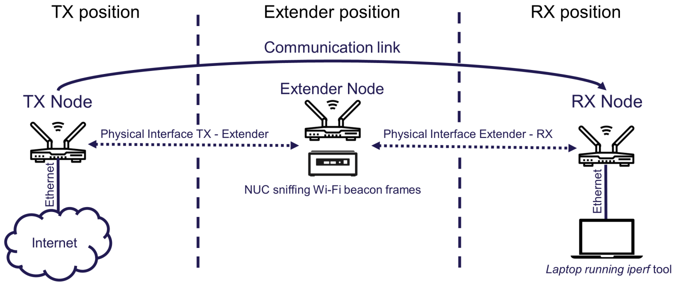

Fig. 1. Schematic of the measurement setup of a mesh network with 3 nodes.

assumption of a mesh network with three nodes, the first one is generally located at the service entry point, which demarcates the Internet service provider domain from the user's internal network. On the other hand, the second and third nodes must be placed so that they can establish communication with each other, and at least one of them must communicate with the first node to create the mesh network. One of the issues in each specific scenario is to define the optimal location of the nodes forming the network. If these nodes are too close to each other, the network range is not maximized due to the overlap between the range of each single node. However, if any of the nodes are too far from those with Internet access within the mesh network, it could degrade its performance due to the difficulty in establishing communication with the rest of the nodes, or they might not be able to establish any connection.

Given these degrees of freedom for positioning the network nodes, this work conducts an empirical evaluation of network performance to define the optimal positioning of the extender nodes in a mesh network. To achieve this, key performance indicator (KPI) parameters related to the received signal and throughput from the network layer perspective are analyzed. From the physical layer standpoint, a study of propagation conditions is also conducted based on five propagation campaigns carried out in three different environments, including offices and houses. Consequently, signal levels for the different bands established in the IEEE 802.11 standards (2.4 GHz, 5 GHz, and 6 GHz) are assessed considering the radio characteristics of the environment, and specific effects such as signal blockage due to obstacles or around-corner propagation are measured. Finally, based on the relationship between the parameters captured for the physical and network layers, some guidelines are elaborated for choosing the optimal location of the network nodes. Note that the state-of-the-art related to Wi-Fi 6E is generally focused on analyzing the point-to-point link between an access point and the user equipment [10], [11]. Additionally, these studies are conducted through the individual analysis of KPIs at the physical layer or the evaluation of throughput at the network layer. In our work, we present (i) the experimental analysis of the Wi-Fi 6E network for three nodes, i.e., a mesh network, where the extender node, defined as an intermediate node in the mesh network, can vary its location, and (ii) the joint analysis of the physical and network layers to determine the optimal placement of our mesh network nodes.

This paper is organized as follows. Section II presents the scenarios and equipment used for the measurement campaigns. Section III describes the analysis from the physical and network layer perspectives, and establishes some guidelines given the KPIs comparison. Finally, Section IV summarises the main conclusions of the work.

II. Measurement Setup

This section presents the scenarios of the indoor measurement campaigns and the methodology followed to determine the optimal location of the nodes in a Wi-Fi 6E mesh network.

A. *Measurement Scenario*

To analyze the performance of these Wi-Fi 6E mesh networks, three different locations where these networks could be potentially deployed have been chosen, and a total of five measurement campaigns have been performed (see Fig. 2). Specifically, the first scenario is an office building (750 m^2) at Aalborg University with a layout consisting of offices, corridors, and office furniture. The second and third scenarios consist of two houses located in residential areas of approximately 170 m^2 and 130 m^2. All three scenarios are strongly conditioned by the presence of obstacles due to the furniture,

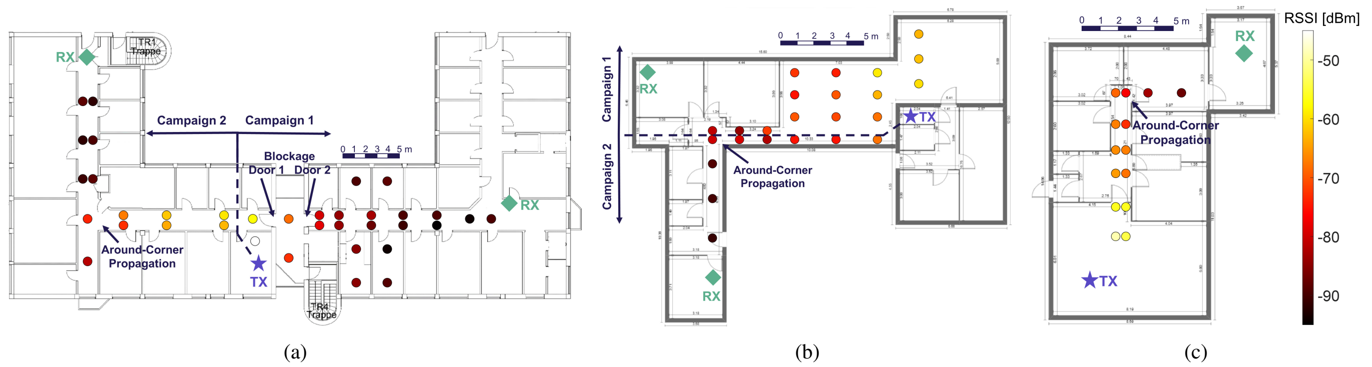

Fig. 2. RSSI values for the TX - Extender link given the different extender node locations: (a) Office building, (b) First house, (c) Second house. Note that in (a) and (b), RSSI is referenced to the single TX node which is common to both campaigns given the scenario. The results correspond to the median RSSI value measured over 30 s in the 6 GHz band following the IEEE 802.11ax standard.

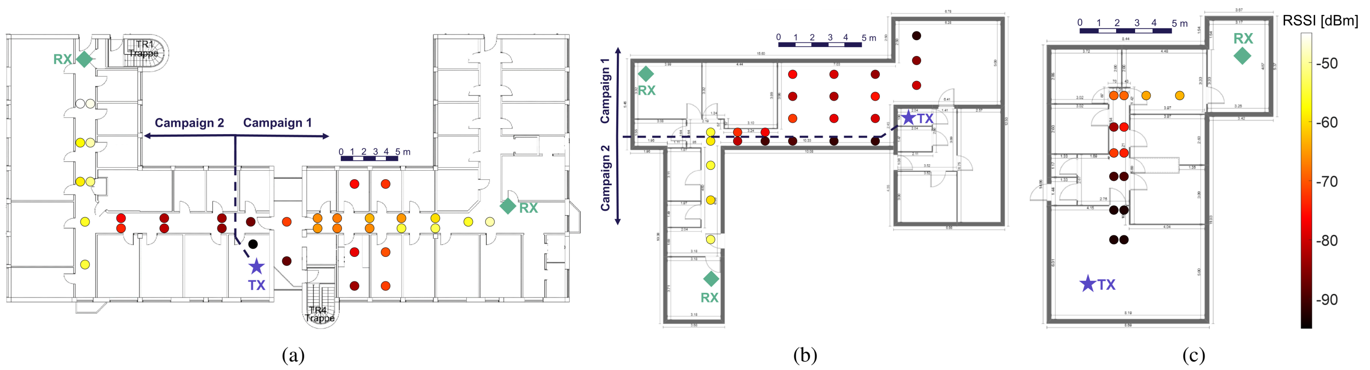

Fig. 3. RSSI values for the RX - Extender link given the different extender node locations: (a) Office building, (b) First house, (c) Second house. Note that in (a) and (b), RSSI is referenced to each of the RX nodes depending on each campaign given the scenario. The results correspond to the median RSSI value measured over 30 s in the 6 GHz band following the IEEE 802.11ax standard.

as well as being prone to blockage due to the multiple walls separating the rooms.

B. *Methodology and Measurement Equipment*

This section details the methodology and the equipment used for analyzing the network conditions and performance. Specifically, three Linksys MX6200 Velop Pro 6E nodes [12] create the mesh network. These nodes are selected since they allow connectivity through the 6 GHz band with Wi-Fi 6E, as well as operating in the 2.4 GHz and 5 GHz bands. Fig. 1 shows a conceptual schematic of the network composed of the three nodes, namely (i) TX, (ii) Extender, and (iii) RX nodes. In the proposed setup, the TX node has Internet connectivity through an Ethernet port, and its position is fixed according to the service entry point. At the other end is the RX node, which is placed in a fixed location where the end-user requires Internet connectivity. For instance, this location could be a room in a house or an office in a business building. If the distance between the TX and RX nodes is too large, it may not be possible to establish connectivity, being necessary to deploy an extender node as a gateway. Therefore, communication within the mesh network occurs between the TX and RX nodes, with a TX - Extender link and a Extender - RX link in the physical layer. Hence, the position of the extender node offers a degree of freedom, as it can affect the network performance based on the physical interface link with the TX and RX nodes.

In order to assess the throughput, a laptop is connected to the RX node through an Ethernet connection. This laptop runs the *iperf* tool, which measures the throughput at the transport layer via the UDP protocol. The same tool is also deployed on an internal server at Aalborg University to generate traffic towards the RX node. A target throughput of 200 Mbps is set due to the maximum data rate provided by the telecom operator in the analyzed networks. The tests, which analyze the downlink from the server to the RX node, evaluate the throughput over 1 s intervals during 30 s per extender node location. In parallel, an Intel NUC12WSHi7 is positioned at the same location as the extender node. This NUC is equipped with an Intel Wi-Fi 6E AX211 network card that operates in the three previously described bands. It is configured to capture 802.11 standard frames from the APs deployed in the environment. Specifically, the beacon frames, broadcasted at a periodicity of 102.4 ms [13], are captured since they provide information regarding the physical layer, such as the signal level of the AP, i.e., the Received Signal Strength Indicator (RSSI). These frames are also captured for 30 s per extender node location. Therefore, it is possible to jointly measure the relationship between the signal strength of the TX and RX nodes with respect to the extender node, and its influence on the throughput.

III. Results

A. *Radio Propagation Analysis*

In this section, we present the measurements and analysis of the mesh network for the three different scenarios. In the first scenario, i.e., the office building illustrated in Fig. 2(a), two different measurement campaigns are performed. In both, the TX node is placed inside an office. In the first campaign, the RX node is placed in a corridor on the west side (23 m TX-RX link), while in the second campaign, the RX node is placed in a corridor on the northwest side (24 m TX-RX link). The first campaign has the particularity that the room to the east of the TX node has two metal doors that block the signal propagation toward the RX node. On the other hand, in the second campaign a right angle appears in the corridor implying around-corner propagation.

In the second scenario, which corresponds to a house shown in Fig. 2(b), the TX node is located in a small technical room where Internet entry access is placed. The first of the measurement campaigns in this scenario involves placing the RX node in a room of the house with a range of 15.5 m, while in the second campaign, the RX node is moved to a room further away where there is also around-corner propagation. Note also that since the TX node is in the small technical room, the signal will be exposed to some blocking.

Finally, in the third scenario presented in Fig. 2(c), the TX is located in the house's living room, while the RX is in a room 14.5 meters away. Due to the presence of multiple walls in the house, the signal relies on propagation along the narrow corridor to reach the RX after turning a corner. All these setups have been chosen such that establishing a connection between the TX and RX nodes is either not feasible due to the range, or if established, the connection is intermittent with data rates below 10 Mbps. Therefore, the presence of the extender node shown previously in Fig. 1 is necessary to improve connectivity. In each campaign, between 9 and 22 candidate locations for the extender node are determined.

Figs. 2(a)-(c) show these positions, and the RSSI on the TX - Extender link for the 6 GHz band. Similarly, Figs. 3(a)-(c) present the RSSI between the RX - Extender link in the 6 GHz band for Wi-Fi 6E. Observing both figures, there is a clear dependence between the distance of the extender node to TX and RX nodes, and the power level in the TX - Extender and RX - Extender links. For short distances and fulfilling Line-of-Sight (LoS) condition, RSSI values are between -45 dBm and -50 dBm, whereas distances larger than 10 meters and Non Line-of-Sight (NLoS) conditions significantly degrade the signal strength. Additionally, given the fixed positions of TX and RX APs, decreasing the distance of the extender to one of the nodes generally means increasing the distance to the other. Therefore, improving the signal on one link inevitably causes some degradation on the other link. Finally, conditions such as signal blockage due to obstacles or around-corner propagation must be considered, as they can cause abrupt drops in signal levels over short distances.

For a quantitative analysis of the path gain (PG) in the 6 GHz band versus the 2.4 GHz and 5 GHz bands, the measurements are modeled according to a generic slope-intercept model:

$$PG(d) = PG_{1m} - 10n\log_{10}(d) + \mathcal{N}\left(0, \sigma^2\right), \quad (1)$$

where PG_{1m} is the intercept term which depicts the path gain at 1 m, n is the slope term that defines the path loss exponent given the distance d, and $\mathcal{N}\left(0, \sigma^2\right)$ is the Gaussian distribution with zero mean and σ standard deviation, which accounts for the large-scale fading in the channel. Given the measured RSSI and the omnidirectional characteristics of the APs, the empirical PG can be obtained directly after adjusting the RSSI values with respect to the transmit power in each of the frequency bands. Therefore, Figs. 4(a) and 4(b) show the empirical values of the path gain for the three frequency bands in two different scenarios. In addition, these measurements have been modeled according to (1). The intercept, slope and standard deviations terms are presented in Table I. The measurements and the intercept model show that the effective range for $f = 2.4$ GHz is larger than that for $f = 5$ GHz and $f = 6$ GHz, with $f = 6$ GHz being the case with the highest path gain. For instance, in Fig. 4(a), the maximum range for a -80 dB path gain is 11.1 m for $f = 2.4$ GHz, while it decreases to 6.1 m for $f = 5$ GHz and 5.0 m for $f = 6$ GHz. This is also observed in the slope-intercept model where $f = 2.4$ GHz has values around $n = 2$, while the two higher frequency cases have path loss exponent values in the approximate range $n \in [3, 4]$. This fact indicates the more

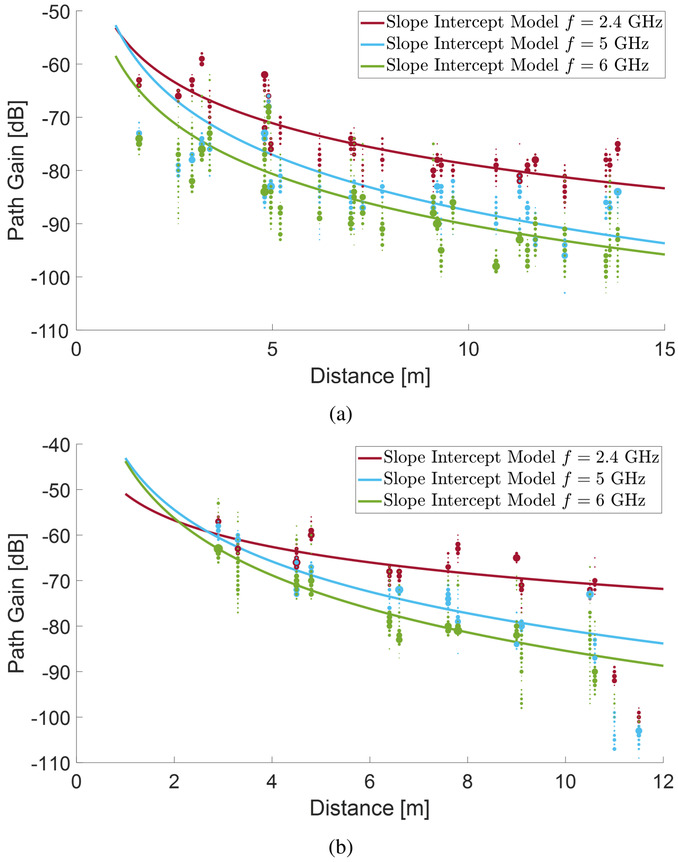

Fig. 4. Path Gain for several distance values given the three frequency bands analyzed: 2.4 GHz, 5 GHz and 6 GHz. (a) First house - Campaign 1, (b) Second house.

TABLE I
GENERIC SLOPE-INTERCEPT MODEL FOR SEVERAL FREQUENCIES WITHIN WI-FI BANDS IN TWO INDOOR SCENARIOS

Measurement Campaign	Frequency	PG_{1m}	n	σ
House 1 - Campaign 1	2.4 GHz	-53.2 dB	2.56	4.4 dB
	5 GHz	-52.7 dB	3.48	4.3 dB
	6 GHz	-58.5 dB	3.17	4.9 dB
House 2	2.4 GHz	-50.9 dB	1.93	3.3 dB
	5 GHz	-43.1 dB	3.77	3.5 dB
	6 GHz	-43.7 dB	4.16	4.8 dB

challenging propagation environment at high frequencies given the signal attenuation due to the scenario condition.

Note that a model such as the slope-intercept model works well in homogeneous environments. However, when faced with specific conditions such as blockage due to an obstacle or around-corner propagation, they are not able to correctly model the path gain trend [14]. For example, the two largest ranges in Fig. 4(b) have not been taken into account for the slope-intercept model fitting as they correspond to around-corner propagation which suffers from a sharp drop in signal strength. To model these effects, we have placed the extender node in those physical locations prone to suffer from strong

TABLE II
AROUND-CORNER PROPAGATION LOSSES FOR SEVERAL FREQUENCIES WITHIN WI-FI BANDS

Measurement Campaign	Reference Link	Frequency	Attenuation
Office - Campaign 2	TX (left turn)	2.4 GHz	7.7 dB
		5 GHz	7.2 dB
		6 GHz	7.0 dB
	TX (right turn)	2.4 GHz	15.1 dB
		5 GHz	13.0 dB
		6 GHz	14.3 dB
	RX	2.4 GHz	13.0 dB
		5 GHz	14.3 dB
		6 GHz	18.7 dB
House 1 - Campaign 2	TX	2.4 GHz	8.0 dB
		5 GHz	15.9 dB
		6 GHz	10.6 dB
	RX	2.4 GHz	21.1 dB
		5 GHz	16.3 dB
		6 GHz	22.2 dB
House 2	TX	2.4 GHz	19.5 dB
		5 GHz	18.0 dB
		6 GHz	14.5 dB
	RX	2.4 GHz	9.9 dB
		5 GHz	7.6 dB
		6 GHz	9.1 dB
Average All Campaigns		2.4 GHz	13.5 dB
		5 GHz	13.2 dB
		6 GHz	13.8 dB

TABLE III
BLOCKAGE LOSSES FOR SEVERAL FREQUENCIES WITHIN WI-FI BANDS

Blockage Source	Frequency	Attenuation
Office - Campaign 1 - Door 1	2.4 GHz	5.0 dB
	5 GHz	11.7 dB
	6 GHz	10.9 dB
Office - Campaign 1 - Door 2	2.4 GHz	6.0 dB
	5 GHz	8.4 dB
	6 GHz	9.4 dB

attenuation due to the geometry of the scenario. In particular, for around-corner propagation, the node has been placed 1 m away on both sides of the corner to evaluate the signal level. Similarly, in blocking situations, the node is placed 1 m before and after the blocking source. Table II presents the around-corner attenuation for the three frequency bands analyzed in several locations within the different scenarios. Median propagation losses over 30 s measurements are shown. At first glance, attenuation values range from 7 dB to 22 dB. Looking at the frequencies given the same location, there is no clear correlation between the three frequencies. However, the comparison between the corners in the different scenarios show significant variability. For example, the attenuation in the second house on the RX - Extender link is around 7-10 dB. However, for the first house and the first campaign, the RX - Extender link suffers an attenuation between 16 and 22 dB. Looking at the geometry of the scenarios in Figs. 2 and 3, the results suggest that the highest attenuations occur in links relying on LoS or obstructed LoS. In contrast, when the signal reaches the corner in an NLoS situation, the losses decrease significantly. This may occur because the NLoS situation involves a strong multipath component at the corner, making it easier to diffract or scatter the signal toward the AP. The average of all around-corner measurements results in propagation losses around 13-14 dB for every frequency. Thus, for around-corner propagation it is essential to take into account the geometry of the scenario to determine the expected losses of the link. Table III illustrates the blockage loss due to presence of walls/metal doors in the office building during the first propagation campaign. In this case, the attenuation values show a clear correlation in terms of the frequency. While 2.4 GHz band presents losses of around 5-6 dB, these values increase to 8-12 dB for 5 GHz and 6 GHz frequency bands, showing that there is a dependence with respect to frequency.

In summary, the results of this section show the attenuation due to signal propagation in the 2.4 GHz, 5 GHz, and 6 GHz

(a) (b) (c)

Fig. 5. Downlink throughput (TP) values for the TX - RX communication link given the different extender node locations: (a) Office building, (b) First house, (c) Second house. The results correspond to the median downlink throughput value measured over 30 s in the 6 GHz band following the IEEE 802.11ax standard.

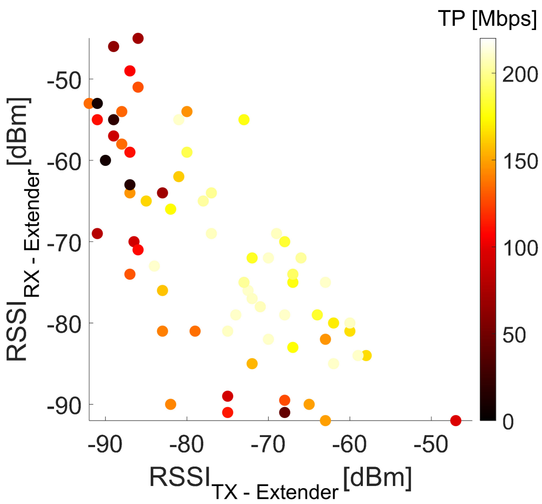

Fig. 6. RSSI values for TX - Extender and RX - Extender links versus downlink throughput measured through the three different scenarios. Measurements correspond to median values for transmissions in each location in the 6 GHz band.

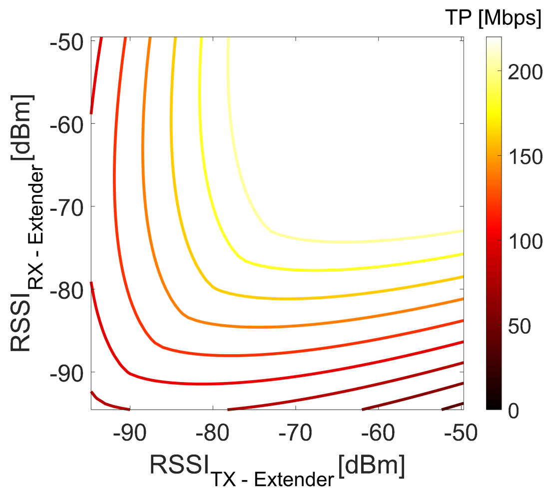

Fig. 7. Regression model for the downlink throughput given the two links that define the physical layer of the Wi-Fi 6E mesh network.

Wi-Fi bands. Emphasis is also placed on the study of specific effects such as signal blockage or propagation around corners. It is observed a significant increase in losses in the analysis of the 5 GHz and 6 GHz bands compared to the 2.4 GHz band, with special emphasis on indoor environments (11.6 dB for a 10-meter range) and blockage situations (4.6 dB). This fact implies a reduction in the effective range of the APs located in the network. Therefore, the use of a mesh network with multiple APs is recommended to increase this range.

B. Throughput Analysis

To evaluate the user experience, as indicated in Fig. 1, the downlink throughput at the RX node is measured in parallel with the RSSI in each scenario given the locations previously described in Figs. 2 and 3. These results are shown in Fig. 5. These values range from 0 to 200 Mbps depending on the location of the extender node. Note that without an extender node, connectivity cannot be established, or at best, it is insufficient for demanding services with a throughput below 10 Mbps. It can be observed that, in general, when the extender node is placed either very close to the TX node or very close to the RX node, the throughput values tend to be low. This is mainly because the signal is not reliably retransmitted, as the signal received at one of the two physical links (see Fig. 1) is poor. However, positioning the extender at an intermediate location between TX and RX generally maximizes the throughput. One exception is found in the first campaign of the first house, where simply placing the extender outside the technical room allows for good signal retransmission between the extender node and RX node, as it avoids the blockage initially introduced by the walls of the room where the TX is located.

To better understand the correlation between the RSSI levels of both physical links and the downlink throughput, Fig. 6 presents a scatter plot where the axes show the RSSI values for the TX - Extender and RX - Extender links, while the color indicates the throughput value obtained for each measurement. It can be seen that when the signal values are maintained above -80 dBm in both links, the throughput tends to be higher. However, as these values decrease, the throughput tends to degrade progressively. Finally, even with values above -60 dBm in the RX - Extender link, the throughput presents values below 30 Mbps because the TX - Extender link is around -90 dBm. Therefore, it can be concluded that as long as both links are above -80 dBm, the throughput values will be high. However, the degradation of only one of the links is sufficient to degrade the overall link performance. Based on these aspects, a simple regression model using only four parameters can be formulated to estimate the throughput through RSSI on both links in a mesh network with three nodes:

$$\text{TP}(\alpha,\beta,\gamma,\delta)[\text{Mbps}] = \alpha + \beta\text{RSSI}_{TX-Sat} + \gamma\text{RSSI}_{RX-Sat} + \delta|\text{RSSI}_{TX-Sat} - \text{RSSI}_{RX-Sat}|^{\zeta}, \quad (2)$$

where α is the intercept term, β and γ model the throughput as a function of the signal strength on the TX - Extender and RX - Extender links, δ is a penalty factor that penalizes the imbalance between the two physical links, and ζ is a term that exponentially adjusts the penalty factor. Intuitively, β and γ influence the individual RSSI of each link, assuming that a higher RSSI value on each link will independently contribute to the throughput. Additionally, as illustrated in Fig. 6, δ introduces a correlation between the two links, such that the throughput is maximized when the signal levels on both links are balanced. Given the scenarios analyzed, the fitting in (2) that reduces the mean square error is performed. For $\zeta = 1.3$, we obtain the following fitting parameters: $\alpha = 640.7$, $\beta = 3.5$, $\gamma = 2.4$ and $\delta = -0.51$. Fig. 7 shows the regression model given the previous parameters. According to the model residuals, the root mean square error is 34.5 Mbps. Hence, based solely on the analysis of the physical link, we can make an initial approximation of the throughput values in the network layer. This fact allows for satisfactorily defining the location of the extender node in the mesh network environment based on the physical layer data.

C. Main findings and recommendations

Based on the extracted results, this subsection outlines a series of guidelines and recommendations for positioning an extender node in a mesh network operating with Wi-Fi 6E. Primarily, it has been experimentally verified that to maximize throughput, the extender node should be approximately at an intermediate location between the TX and RX nodes. This is due to the fact that, otherwise, one of the physical links might be degraded worsening the signal retransmission conditions. According to the throughput measurements performed in indoor NLoS environments such as offices or houses, the minimum signal required to ensure a stable connection is given for RSSI values around -80 dBm (Path Gain of -94 dB for an EIRP of 14 dBm). Following the guidelines established by the slope-intercept model for $f = 6$ GHz, empirical measurements show that the maximum range for these path gain values is around 13 to 16 meters. However, obstacles in the channel or specific scenario geometries, such as around-corner propagation, may imply additional losses. In particular, it has been observed that blockage losses have a strong correlation with frequency, so they should preferably be avoided when positioning the APs as they will have a greater effect on Wi-Fi 6E. On the other hand, around-corner losses are more related to the physical arrangement of the APs than to frequency, with a multipath environment being more favorable for overcoming this effect. Based on the previous findings, the following recommendations are outlined:

- The best network performance is achieved when the physical links are balanced in terms of RSSI with values above -80 dB. In the case of LoS between the extender and both TX and RX nodes, the node should be placed at an equidistant position between them.
- For cases where one of the nodes is in NLoS with respect to the extender, it is recommended to reduce the range between the extender and this NLoS node to minimize the attenuation in this link.
- The maximum range between nodes should not exceed 15 m in NLoS conditions, and should be progressively reduced in the presence of walls or corners.
- Between two adjacent nodes, more than one source of obstruction should be avoided to ensure adequate RSSI.

IV. Conclusion

This paper presents an experimental evaluation of a Wi-Fi 6E mesh network through several measurement campaigns in three different scenarios to define the optimal placement of the extender nodes in a mesh network. In particular, given a set of three nodes, the effect of the location of the intermediate node is analyzed under the assumption that the TX and RX nodes are fixed. Thus, the optimal location of the intermediate node is analyzed based on physical layer KPIs and their comparison with the network performance. To define this location, the analysis includes a study from the physical layer point of view with emphasis on the signal level in the TX - Extender and RX - Extender links for the three bands where Wi-Fi currently operates, i.e., 2.4 GHz, 5 GHz and 6 GHz. The results show a clear decrease in the effective range for 6 GHz versus 2.4 GHz. Therefore, the need to employ mesh networks for Wi-Fi 6E deployment becomes evident for large ranges. Hence, an analysis of the downlink throughput in the different scenarios is performed and the relationship between signal strength and data rate is evaluated. Finally, based on the extracted results, some recommendations are summarized to determine the optimal location conditions of the extender node in the mesh network. Thus, the analysis presented in this work provides insights into the performance of a three-node mesh network, serving as an initial approach to studying a broader range of more complex mesh network topologies in future work.

References

[1] K. Pahlavan and P. Krishnamurthy, "Evolution and Impact of Wi-Fi Technology and Applications: A Historical Perspective", *International Journal of Wireless Information Networks*, vol. 28, no. 1, pp. 3–19, 2021.

[2] B. P. Crow, I. Widjaja, J. G. Kim and P. T. Sakai, "IEEE 802.11 Wireless Local Area Networks," *IEEE Communications Magazine*, vol. 35, no. 9, pp. 116-126, 1997.

[3] S. Chieochan, E. Hossain and J. Diamond, "Channel assignment schemes for infrastructure-based 802.11 WLANs: A survey," *IEEE Communications Surveys & Tutorials*, vol. 12, no. 1, pp. 124-136, 2010.

[4] S. Lindroos, A. Hakkala and S. Virtanen, "Battle of the Bands: A Long-Term Analysis of Frequency Band and Channel Distribution Development in WLANs," *IEEE Access*, vol. 10, pp. 61463-61471, 2022.

[5] E. Khorov, A. Kiryanov, A. Lyakhov and G. Bianchi, "A Tutorial on IEEE 802.11ax High Efficiency WLANs," *IEEE Communications Surveys & Tutorials*, vol. 21, no. 1, pp. 197-216, 2019.

[6] G. Naik, J. -M. Park, J. Ashdown and W. Lehr, "Next Generation Wi-Fi and 5G NR-U in the 6 GHz Bands: Opportunities and Challenges," *IEEE Access*, vol. 8, pp. 153027-153056, 2020.

[7] V. Deniau, C. Gransart, G. L. Romero, E. P. Simon and J. Farah, "IEEE 802.11n Communications in the Presence of Frequency-Sweeping Interference Signals," *IEEE Transactions on Electromagnetic Compatibility*, vol. 59, no. 5, pp. 1625-1633, 2017.

[8] *Study on channel model for frequencies from 0.5 to 100 GHz (Release 17)*, 3GPP Standard TR38.901 V17.0.0, 2022.

[9] B. Gokalgandhi, M. Tavares, D. Samardzija, I. Seskar and H. Gacanin, "Reliable Low-Latency Wi-Fi Mesh Networks," *IEEE Internet of Things Journal*, vol. 9, no. 6, pp. 4533-4553, 2022.

[10] S. Dogan-Tusha, A. Tusha, H. Nasiri, M. I. Rochman and M. Ghosh, "Indoor and Outdoor Measurement Campaign for Unlicensed 6 GHz Operation with Wi-Fi 6E," in *2023 26th International Symposium on Wireless Personal Multimedia Communications (WPMC)*, Tampa, FL, USA, pp. 1-6, 2023.

[11] H. Brunner, M. Stocker, M. Schuh, M. Schuß, C. A. Boano and K. Römer, "Understanding and Mitigating the Impact of Wi-Fi 6E Interference on Ultra-Wideband Communications and Ranging," in *2022 21st ACM/IEEE International Conference on Information Processing in Sensor Networks (IPSN)*, Milano, Italy, pp. 92-104, 2022.

[12] Linksys MX6200 Velop Pro 6E. [Online]. Available: https://www.linksys.com/support-article?articleNum=50943

[13] "IEEE Standard for Information Technology–Telecommunications and Information Exchange between Systems - Local and Metropolitan Area Networks–Specific Requirements - Part 11: Wireless LAN Medium Access Control (MAC) and Physical Layer (PHY) Specifications," *IEEE Std 802.11-2020 (Revision of IEEE Std 802.11-2016)* pp. 1-4379, 2021.

[14] D. Chizhik *et al.*, "Directional Measurements and Propagation Models at 28 GHz for Reliable Factory Coverage," *IEEE Transactions on Antennas and Propagation*, vol. 70, no. 10, pp. 9596-9606, 2022.